Direct Observation of Ge and Si Ordering at the Si/B/Ge_xSi_{1-x}(111) Interface by Anomalous X-Ray Diffraction

D. J. Tweet, K. Akimoto, and T. Tatsumi
Microelectronics Research Laboratories, NEC Corporation, 34 Miyukigaoka, Tsukuba, Ibaraki 305, Japan

I. Hirosawa and J. Mizuki
Fundamental Research Laboratories, NEC Corporation, 34 Miyukigaoka, Tsukuba, Ibaraki 305, Japan

J. Matsui
Research and Development Group, NEC Corporation, 34 Miyukigaoka, Tsukuba, Ibaraki 305, Japan
(Received 23 March 1992)

We have modified multiple-wavelength anomalous dispersion, a powerful direct method, and applied it for the first time to an interface. This allows us to separate heavy and light atoms, and so deduce the structure. We find that at the Si/B$(\sqrt{3}\times\sqrt{3})R30°$/$Ge_xSi_{1-x}$(111) interface Ge and Si atoms occupy separate sites. Boron is in a substitutional site with four Si nearest neighbors and the other positions are dominated by Ge. This ordering may be due to chemical (binding-energy) effects combined with a kinetic, surface-strain mechanism related to one proposed for the ordered GeSi(001) system.

PACS numbers: 68.35.Bs, 61.10.My, 68.55.Bd, 68.55.Ln

In recent years there have been a number of studies of the B$(\sqrt{3}\times\sqrt{3})R30°$/Si(111) surface [1–4] [abbreviated B$\sqrt{3}$/Si(111)] and the Si/B$\sqrt{3}$/Si(111) interface [3,4]. The motivation has been the desire to create a new class of so-called δ-doped materials, in which holes produced by boron are trapped at the two-dimensional interface.

Unlike other group-III elements on the Si(111) surface, boron is found to substitute for one of the Si atoms, resulting in a very stable structure. However, because of the small size of boron, the four surrounding Si atoms must shift appreciably towards it. Tatsumi *et al.* [5] reasoned that including Ge in the system should partially relieve some of the strain, since Ge is larger than both Si and boron, resulting in an even more stable interface. In addition, band bending at the Si/B$\sqrt{3}$/Ge_xSi_{1-x}(111) interface due to the different band gaps of Si and Ge_xSi_{1-x} should improve the hole-trapping properties. The purpose of the present work is to determine the structure of Si/B$\sqrt{3}$/Ge_xSi_{1-x}(111) and understand the reasons for its atomic arrangement.

We report here clear, direct evidence for ordering of the Ge and Si atoms at this interface. Specifically, we find that boron lies in a substitutional site surrounded by four nearest-neighbor Si atoms with Ge in the other sites. For several years there has been much interest in the ordering of GeSi alloys grown along the [001] orientation [6–8]. The ordering we observe may be partly due to a surface-stress mechanism related to one proposed for the GeSi(001) system [7]. Yet this stress mechanism alone appears insufficient to explain the structure; chemical effects, i.e., the binding-energy difference between the B-Si and B-Ge bonds, may play the remaining key role.

This structure was derived by applying a direct method to anomalous x-ray diffraction data. This technique, known as multiple-wavelength anomalous dispersion (MAD) [9], has been successfully used in protein crystallography for about ten years [10], and we have made appropriate modifications to facilitate its use in studying surfaces and interfaces. We were motivated by the ability of MAD to separate out heavier atoms and by recent observations of anomalous dispersion effects at an interface [11]. Such effects alone can provide direct information about an interface, such as the registry of an overlayer with the substrate [12]. Here we describe the first application of MAD to the analysis of an interfacial superstructure, resulting in model-independent evidence of ordering. To obtain these results, synchrotron radiation was used to measure the integrated intensities of ten $\sqrt{3}$ reflections as a function of energy across the Ge K-shell absorption edge. From the MAD analysis of these data, separate partial Patterson maps (the electron density-density correlation function) for Si and for Ge were generated. These Patterson maps have distinct differences, immediately providing direct evidence of ordering. These maps then led to a structural model which was refined by fitting to the data.

To prepare the sample, 20 Å of Ge was deposited on a Si(111)7×7 substrate held at a temperature (T_{sub}) of 630 °C, resulting in a 5×5 pattern. Studies of similar systems [13,14] indicate that at this point the surface has a dimer-adatom-stacking-fault structure consisting of mostly Ge in the adatom and (possibly) stacking-fault layers with intermixing of Ge and Si beneath. Next, $\frac{1}{3}$ monolayer of boron was deposited from an HBO_2 Knudsen cell, again at T_{sub}=630 °C, resulting in a $(\sqrt{3}\times\sqrt{3})R30°$ pattern. The sample was capped by 100 Å of epitaxial Si, as indicated by reflection high-energy electron diffraction, grown at T_{sub}=400 °C.

The experiment was performed at beam line 9C in the Photon Factory of the National Laboratory for high Energy Physics (KEK) in Tsukuba, Japan, using grazing-incidence diffraction (GID) techniques. The intensity of

© 1992 The American Physical Society

each reconstructed reflection was determined by measuring a rocking curve and taking the background-subtracted integrated intensity of the peak, after normalizing to monitor counts.

Initially, measurements of $\sqrt{3}$ reflections were made at just two x-ray energies, at $E=11.098\pm0.002$ keV, near the Ge K-shell absorption edge of $E_{\text{edge}}=11.104$ keV (Fig. 1), and at $E=8.266\pm0.002$ keV, far from the edge (not shown). In Fig. 1, the area of each circle is proportional to the observed intensity after correcting for polarization, Lorentz factor, and variation of the active sample area. The uncertainties were taken from multiple measurements of equivalent reflections, but were set to at least 10%, typical of GID experiments. Also, the data have been averaged about mirror planes observed along the $[\bar{4}22]$ and $[\bar{2}\bar{2}4]$ directions. The difference in intensities between the left- and right-hand sides of the figure is due to a small component of the momentum transfer perpendicular to the interface. The large differences observed indicate that several layers are involved in this reconstruction.

The second set of data consists of intensity measurements of ten $\sqrt{3}$ reflections (two of which are equivalent) at 31 values of the x-ray energy across E_{edge}. Representative scans are shown in Fig. 2. Besides the corrections used on the data of Fig. 1, several additional factors are required: the energy-dependent part of the Lorentz correction, the air absorption, and the relative efficiency of the ionization chamber monitor.

The strong variation in intensity seen in Fig. 2 is due to the so-called anomalous terms, f' and f'', in the atomic form factor of Ge,

$$f_{\text{Ge}}(\mathbf{h},E)=f^{n}_{\text{Ge}}(\mathbf{h})+f'(E)+if''(E)\,. \tag{1}$$

Here f^{n}_{Ge} is the normal part which depends only on $\mathbf{h}$, the momentum transfer of the (hkl) reflection. Most of our data look like Fig. 2(a) which shows a strong peak that decreases in intensity near E_{edge}, but notice that Fig. 2(b) shows a very weak reflection that *increases* in intensity.

These sort of data lend themselves very well to analysis by MAD. This technique consists of separating the total structure factor $F(\mathbf{h},E)$ into normal and anomalous parts: Define the magnitude $|F^{n}_{1}(\mathbf{h})|$ and phase $\phi^{n}_{1}(\mathbf{h})$ of the structure factor for the normally scattering atoms (boron and Si), as well as the corresponding terms $|F^{n}_{2}(\mathbf{h})|$ and $\phi^{n}_{2}(\mathbf{h})$ for the *normal* part of the structure factor for the anomalously scattering atoms (Ge). The anomalous terms are gathered into coefficients $p_1(\mathbf{h},E)$, $p_2(\mathbf{h},E)$, and $p_3(\mathbf{h},E)$. The intensity versus energy data for a given peak $\mathbf{h}$ are then proportional to [9]

$$\begin{aligned}|F(\mathbf{h},E)|^2=&|F^{n}_{1}(\mathbf{h})|^2+p_1(\mathbf{h},E)|F^{n}_{2}(\mathbf{h})|^2\\&+p_2(\mathbf{h},E)[|F^{n}_{1}(\mathbf{h})|^2|F^{n}_{2}(\mathbf{h})|^2]^{1/2}\cos\Delta\phi(\mathbf{h})\\&+p_3(\mathbf{h},E)[|F^{n}_{1}(\mathbf{h})|^2|F^{n}_{2}(\mathbf{h})|^2]^{1/2}\sin\Delta\phi(\mathbf{h})\,,\end{aligned} \tag{2}$$

where $\Delta\phi(\mathbf{h})\equiv\phi^{n}_{1}(\mathbf{h})-\phi^{n}_{2}(\mathbf{h})$.

Calculating p_1, p_2, and p_3 from tables of f' and f'' [15], Eq. (2) is then fitted to the data illustrated in Fig. 2 by treating $|F^{n}_{1}(\mathbf{h})|^2$, $|F^{n}_{2}(\mathbf{h})|^2$, and $\Delta\phi(\mathbf{h})$ as parameters in a nonlinear least-squares fitting program. (An average Debye-Waller factor was first removed from the data.) This is a modification of the usual MAD technique for

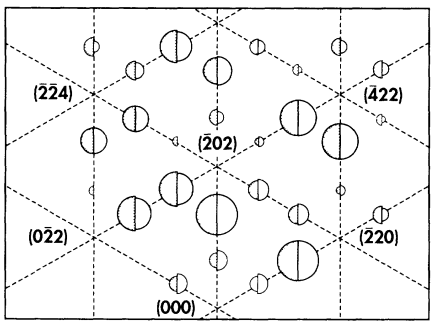

FIG. 1. Intensity map of diffraction from the reconstructed interface measured at an x-ray energy of $E=11.098$ keV. The dotted lines cross at the bulk fundamental lattice points, several of which are identified. The shaded left half circles show the measured intensities and the right half circles show the values calculated from the model structure of Fig. 4.

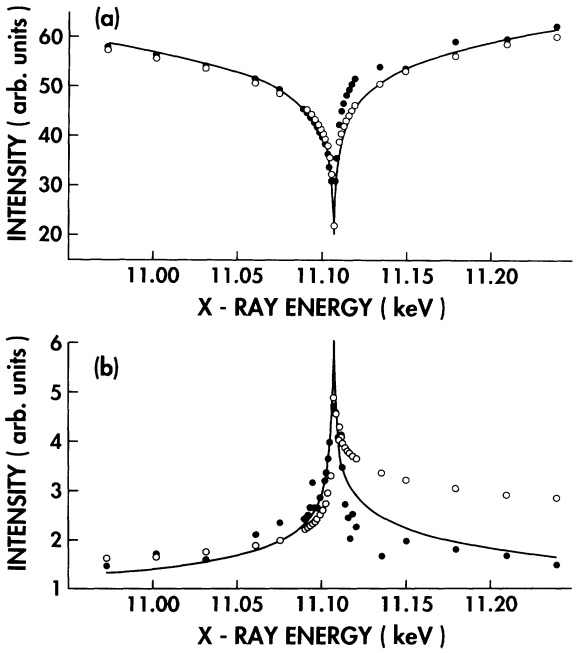

FIG. 2. Representative scans of intensity vs E for the reconstructed peaks (a) $(hkl)=\frac{2}{3}(\bar{2}20)$ and (b) $(hkl)=\frac{4}{3}(\bar{2}20)$. The data (solid circles) are the average of three scans for (a) and four scans for (b). The line is the fit by the MAD analysis [Eq. (2)]. The open circles are the fit with the model structure shown in Fig. 4. The XAFS-like oscillation just beyond E_{edge} in the data of part (a) was not included in either fit.

protein crystallography in which the thousands of accessible diffraction peaks are measured at just a few energies. For a given peak, Eq. (2) is then evaluated at each of these values of E and the parameters extracted by solving as a set of linear equations [9]. In comparison, interfaces give far fewer accessible peaks, but by measuring each at many values of E and fitting as described above, we obtain good results.

From the resulting set of $|F_1^n(\mathbf{h})|^2$ and $|F_2^n(\mathbf{h})|^2$ and using the $p31m$ symmetry of the $\sqrt{3}$ unit cell we generated separate partial Patterson maps for boron and Si, Fig. 3(a), and for Ge, Fig. 3(b), respectively. (Since boron has less than half as many electrons as Si, the boron-Si map is strongly dominated by Si.) The peak-origin distances indicate the in-plane atomic separations. The maps are quite different, providing direct, model-independent evidence that Ge and Si occupy different sites.

The main peaks in the maps reveal that the Si-Si and Ge-Ge in-plane distances are noticeably smaller and larger than the unreconstructed length, respectively, although the distortion is significantly greater for Si. Interpreting the maps based on the in-plane hexagon shown in Fig. 3(c) it is apparent that the main Si peak is due to the AB pair of sites while the smaller peak along $[1\bar{1}0]$ is due to BB. The Ge peak is then due to CD with possibly some contribution from CB (if site B is not all Si).

This interpretation leads to the model shown in Fig. 4. This model was refined by fitting to all the data represented in Figs. 1 and 2, in which the results of the best fit ($\chi^2=2.4$) are also plotted [16]. The fits are quite good, and even reproduce the observed increase in intensity at E_{edge} of Fig. 2(b). We find that the boron is in a Si substitutional site [17] [site A, the center of the distortion in Fig. 3(c)], and prefers to be surrounded by four Si nearest-neighbor atoms (site "1" also has 10% Ge distorted 0.10 Å), with the other sites Ge, except for the Si overlayer. Uncertainties in composition are $\pm 30\%$ for sites 4 and 5 and $\pm 10\%$ for the rest. Atomic positions normal to the interface were estimated by a bond-length-preserving calculation. Note that both the boron site and the distortion of the first layer Si are the same as in the B$\sqrt{3}$/Si(111) system [1-4], while the distortions in layers 4 and 5 are not; they are small or nonexistent in B$\sqrt{3}$/Si(111).

At first, this structure appears counterintuitive. As a result of size considerations one might expect that boron should be surrounded by Ge, not Si; there is indirect evidence that in bulk, this is the case [18]. Also, ordered GeSi(001) alloys have been studied for some time [6-8]. Although a matter of debate, one proposed mechanism [7] involves a stress field induced by surface dimers, in which sites under compressive and tensile stress are occupied by Si and Ge, respectively. As the alloy is grown at low temperatures this structure is then "frozen in," resulting in long-range ordering.

It has been suggested [19] that a similar kinetic, surface-stress mechanism may be at work in the present system: In analogy with B$\sqrt{3}$/Si(111), when the B$\sqrt{3}$/Ge_xSi_{1-x}(111) surface initially forms, the T_4 adatom site above the boron should be occupied [1,2,4]. Such a T_4 adatom would put the atoms in site 1 in Fig. 4 under compressive stress, favoring Si, as observed. (The situation for the 3a atom is less clear, due to the small size of the boron above it.) Low-temperature overlayer growth

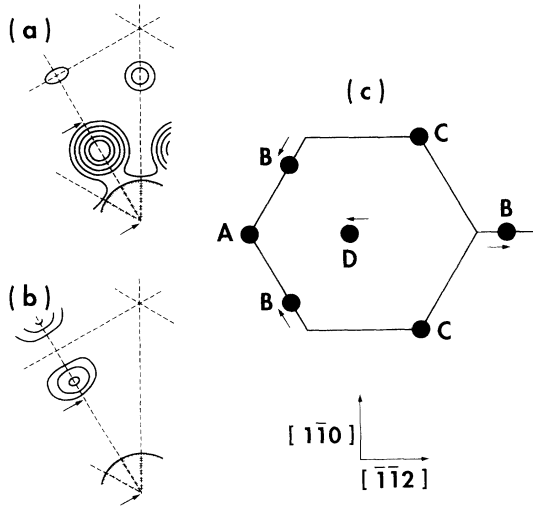

FIG. 3. Partial Patterson maps for (a) boron and Si and for (b) Ge. Only positive contours are shown. The contour spacing is 10 times larger in (b) than in (a) while the shaded peak at the origin rises 17 levels above zero in both cases. Arrows indicate the unreconstructed in-plane bond length. From these maps the distorted hexagon in (c) is inferred with the composition of sites A, B, C, and D discussed in the text.

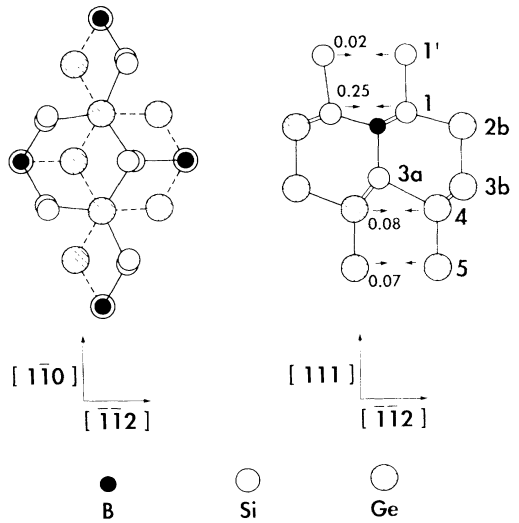

FIG. 4. Model structure of the interface viewed from above (left) and the side (right). The top view shows the entire $(\sqrt{3}\times\sqrt{3})R30°$ unit cell, while the side view shows the structure near one boron atom. In-plane distortions are indicated in units of Å (± 0.02 Å).

would remove the adatom [4] but leave the ordering intact.

However, if this were the only important mechanism, the presence of boron would be incidental to the ordering. Yet, as noted above, before boron is added to the GeSi(111)(5×5) surface no similar ordering is observed. Boron, or the $\sqrt{3}$ reconstruction it induces, is critical. Since boron's small size would seem to favor a structure opposite to that observed, the answer may lie in its chemistry: From trends in the periodic table the B-Si binding energy should be greater than that for B-Ge. Combined with the surface stress field, this may produce the observed ordering.

In summary, we report the first application of the MAD analysis technique to an interfacial superstructure and find direct evidence of ordering. This method is very powerful and should prove useful in the analysis of other compound surfaces and interfaces. In the Si/B$\sqrt{3}$/Ge_xSi_{1-x}(111) interface the boron sits in a Si substitutional site surrounded by four Si nearest-neighbor atoms with Ge in the remaining sites. This structure may be determined by a combination of chemical (binding energy) and kinetic (surface stress field) effects.

We would like to thank S. Kimura, T. W. Ebbesen, Y. Miyamoto, and A. Oshiyama for useful discussions. The cooperation of the members of the Photon Factory (KEK) is also gratefully acknowledged.

[1] P. Bedrossian, R. D. Meade, K. Mortensen, D. M. Chen, J. A. Golovchenko, and D. Vanderbilt, Phys. Rev. Lett. **63**, 1257 (1989).

[2] I.-W. Lyo, E. Kaxiras, and Ph. Avouris, Phys. Rev. Lett. **63**, 1261 (1989).

[3] K. Akimoto, J. Mizuki, I. Hirosawa, T. Tatsumi, H. Hirayama, N. Aizaki, and J. Matsui, in *Extended Abstracts of the Nineteenth Conference on Solid State Devices and Materials* (Business Center for Academic Societies, Tokyo, 1987), p. 463; K. Akimoto, I. Hirosawa, T. Tatsumi, H. Hirayama, J. Mizuki, and J. Matsui, Appl. Phys. Lett. **56**, 1225 (1990).

[4] R. L. Headrick, I. K. Robinson, E. Vlieg, and L. C. Feldman, Phys. Rev. Lett. **63**, 1253 (1989).

[5] T. Tatsumi, I. Hirosawa, T. Niino, H. Hirayama, and J. Mizuki, Appl. Phys. Lett. **57**, 1395 (1990).

[6] A. Ourmazd and J. C. Bean, Phys. Rev. Lett. **55**, 765 (1985).

[7] P. C. Kelires and J. Tersoff, Phys. Rev. Lett. **63**, 1164 (1989); F. K. LeGoues, V. P. Kesan, S. S. Iyer, J. Tersoff, and R. Tromp, *ibid.* **64**, 2038 (1990).

[8] D. E. Jesson, S. J. Pennycook, J.-M. Baribeau, and D. C. Houghton, Phys. Rev. Lett. **68**, 2062 (1992).

[9] J. Karle, Int. J. Quantum Chem. **7**, 357 (1980); for a review, see J. Karle, Phys. Today **42**, No. 6, 22 (1989).

[10] W. A. Hendrickson and M. M. Teeter, Nature (London) **290**, 107 (1981).

[11] K. Akimoto, K. Hirose, and J. Mizuki, Phys. Rev. B **44**, 1622 (1991).

[12] F. J. Walker, E. D. Specht, and R. A. McKee, Phys. Rev. Lett. **67**, 2818 (1991).

[13] See K. Kajiyama, Y. Tanishiro, and K. Takayanagi, Surf. Sci. **222**, 47 (1989), and references therein.

[14] See J. C. Woicik and P. Pianetta, in *Synchrotron Radiation Research: Advances in Surface and Interface Science, Volume 2*, edited by R. Z. Bachrach (Plenum, New York, 1992), p. 211, and references therein.

[15] S. Sasaki, KEK Report No. 88-14, 1989 (unpublished).

[16] Bulk Debye-Waller factors of 0.45 and 0.6 $Å^2$ were used for Si and Ge, respectively, while 0.5 $Å^2$ was used for boron.

[17] The alternative boron sites B-T_4 and B-H_3 gave poor fits to the data and were rejected.

[18] H. Hirayama, T. Tatsumi, and N. Aizaki, Appl. Phys. Lett. **52**, 1335 (1988).

[19] R. M. Tromp (private communication).

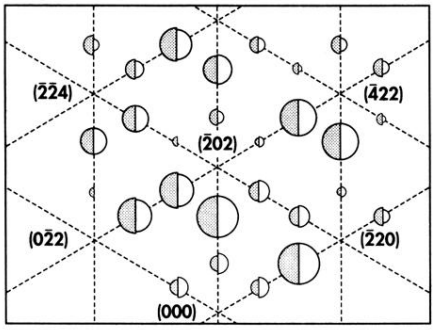

FIG. 1. Intensity map of diffraction from the reconstructed interface measured at an x-ray energy of $E = 11.098$ keV. The dotted lines cross at the bulk fundamental lattice points, several of which are identified. The shaded left half circles show the measured intensities and the right half circles show the values calculated from the model structure of Fig. 4.

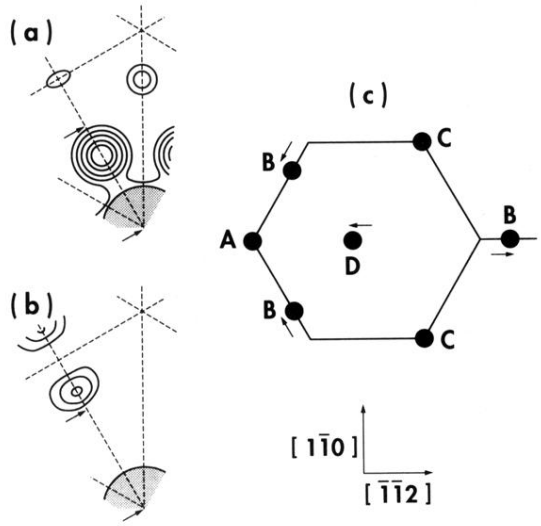

FIG. 3. Partial Patterson maps for (a) boron and Si and for (b) Ge. Only positive contours are shown. The contour spacing is 10 times larger in (b) than in (a) while the shaded peak at the origin rises 17 levels above zero in both cases. Arrows indicate the unreconstructed in-plane bond length. From these maps the distorted hexagon in (c) is inferred with the composition of sites *A*, *B*, *C*, and *D* discussed in the text.